

A Semiactive Vibration Control Design for Suspension Systems with Mr Dampers

Hamid Reza Karimi

*Department of Engineering, Faculty of Engineering and Science
University of Agder
Norway*

1. Introduction

In an automotive system, the vehicle suspension usually contributes to the vehicle's handling and braking for good active safety and driving pleasure and keeps the vehicle occupants comfortable and reasonably well isolated from road noise, bumps and vibrations. The design of vehicle suspension systems is an active research field in automotive industry (Du and Zhang, 2007; Guglielmino, *et al.*, 2008). Most conventional suspensions use passive springs to absorb impacts and shock absorbers to control spring motions. The shock absorbers damp out the motions of a vehicle up and down on its springs, and also damp out much of the wheel bounce when the unsprung weight of a wheel, hub, axle and sometimes brakes and differential bounces up and down on the springiness of a tire.

Semiactive suspension techniques (Karkoub and Dhabi, 2006; Shen, *et al.*, 2006; Zapateiro, *et al.*, 2009) promise a solution to the problem of vibration absorption with some comparatively better features than active and passive devices. Compared with passive dampers, active and semiactive devices can be tuned due to their flexible structure. One of the drawbacks of active dampers is that they may become unstable if the controller fails. On the contrary, semiactive devices are inherently stable, because they cannot inject energy to the controlled system, and will act as pure passive dampers in case of control failure. Among semiactive control devices, magnetorheological (MR) dampers are particularly interesting because of the high damping force they can produce with low energy requirements (being possible to operate with batteries), simple mechanical design and low production costs. The damping force of MR dampers is produced when the MR fluid inside the device changes its rheological properties in the presence of a magnetic field. In other words, by varying the magnitude of an external magnetic field, the MR fluid can reversibly go from a liquid state to a semisolid one or vice versa (Carlson, 1999). Despite the above advantages, MR dampers have a complex nonlinear behavior that makes modeling and control a challenging task. In general, MR dampers exhibit a hysteretic force - velocity loop response whose shape depends on the magnitude of the magnetic field and other variables. Diverse MR damper models have been developed for describing the nonlinear dynamics and formulating the semiactive control laws (Dyke, *et al.*, 1998; Zapateiro and Luo, 2007; Rodriguez, *et al.*, 2009). Most of the MR damper's models found in literature are the so-called phenomenological models which are based on the mechanical behavior of the device (Spencer, *et al.*, 1997; Ikhouane and Rodellar, 2007).

The objective of the work is to mitigate the vibration in semiactive suspension systems equipped with a MR damper. Most conventional suspensions use passive devices to absorb impacts and vibrations, which is generally difficult to adapt to the uncertain circumstances. Semiactive suspension techniques promise a solution to the above problem with some comparatively better features than active and passive suspension devices. To this aim, a backstepping control is proposed to mitigate the vibration in this application. In the design of backstepping control, the Bouc-Wen model of the MR damper is used to estimate the damping force of the semiactive device taking the control voltage and velocity inputs as variables and the semiactive control law takes into account the hysteretic nonlinearity of the MR damper. The performance of the proposed semiactive suspension strategy is evaluated through an experimental platform for the semiactive vehicle suspension available in our laboratory.

The chapter is organized as follows. In the section 2, physical study of MR dampers is proposed. The mathematical model for the semiactive suspension experimental platform is introduced in the section 3. In the section 4, details on the formulation of the backstepping control are given. The results of control performance verification are presented and discussed in the section 5. Finally, conclusions are drawn at the end of the paper.

2. MR damper

Nowadays dampers based on MagnetoRheological (MR) fluids are receiving significant attention especially for control of structural vibration and automotive suspension systems. . In most cases it is necessary to develop an appropriate control strategy which is practically implementable when a suitable model of MR damper is available. It is not a trivial task to model the dynamic of MR damper because of their inherent nonlinear and hysteretic dynamics. In this work, an alternative representation of the MR damper in term of neural network is developed. Training and validating of the network models are achieved by using data generated from the numerical simulation of the nonlinear differential equations proposed for MR damper. The MR damper is a controllable fluid damper which belongs in the semi-active category. A brief overview of the physical buildup of an MR damper is seen in this section.

2.1 Physical study

The MR damper has a physical structure much like a typical passive damper: an outer casing, piston, piston rod and damping fluid confined within the outer casing. The main difference lies in the use of MR fluid and an electromagnet.

2.1.1 MR fluid

A magneto rheological fluid is usually a type of mineral or silicone oil that carries magnetic particles. These magnetic particles may be iron particles that can measure 3-10 microns in diameter, shown in Fig. 1. In addition to these particles it might also contain additives to keep the iron particles suspended. When this fluid is subject to a magnetic field the iron particles behave like dipoles and start aligning along the constant flux, shown in Fig. 2. When the fluid is contained between the dipoles, its movement is restricted by the chain of the particles thus increasing its viscosity. Thus it changes its state from liquid to a viscoelastic solid.

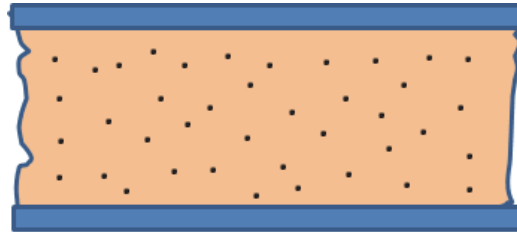


Fig. 1. Magnetic particles in the MR fluid.

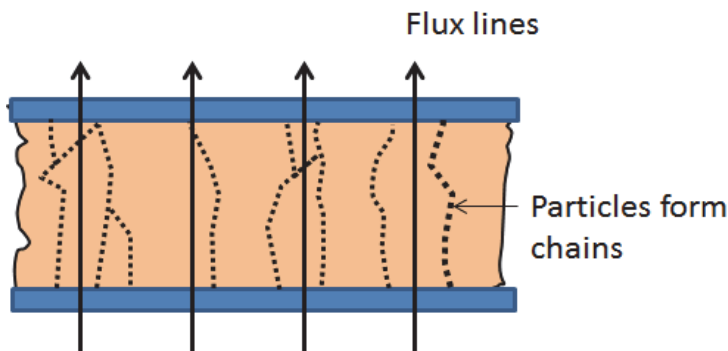


Fig. 2. Particles aligning along the flux lines.

Mechanical properties of the fluid in its 'on' state are anisotropic i.e. it is directly dependent on the direction. Hence while designing a MR device it is important to ensure that the lines of flux are perpendicular to the direction of the motion to be restricted. This way the yield stress of the fluid can be controlled very accurately by varying the magnetic field intensity. Controlling the yield stress of a MR fluid is important because once the peak of the yield stress is reached the fluid cannot be further magnetized and it can result in shearing. It is also known that the MR Fluids can operate at temperatures ranging from -40 to 150° C with only slight changes in the yield stress. Hence it is possible to control the fluids ability to transmit force with an electromagnet and make use of it in control-based applications.

2.1.2 Electromagnet

The electromagnet in the MR damper can be made with coils wound around the piston. An example is the MR damper design by Gavin et. al (2001), seen in Fig. 3. The wire connecting this electromagnet is then lead out through the piston shaft.

2.2 Modes of operation

MR Fluids can be used in three different modes (Spencer et al, 1997):

Flow mode: Fluid is flowing as a result of pressure gradient between two stationary plates. It can be used in dampers and shock absorbers, by using the movement to be controlled to force the fluid through channels, across which a magnetic field is applied, see Fig. 4.

Shear mode: In this mode the fluid is between two plates moving relative to one another. It is used in clutches and brakes i.e. in places where rotational motion must be controlled, see Fig. 5.

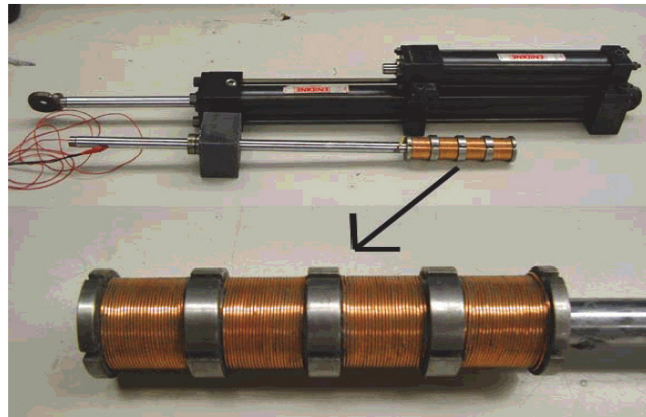


Fig. 3. Electromagnetic piston.

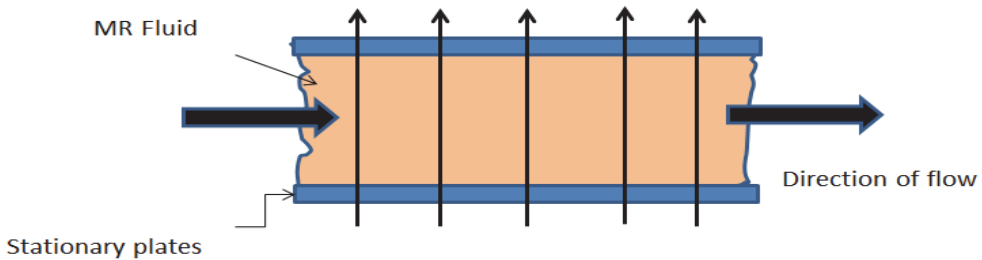


Fig. 4. Flow mode.

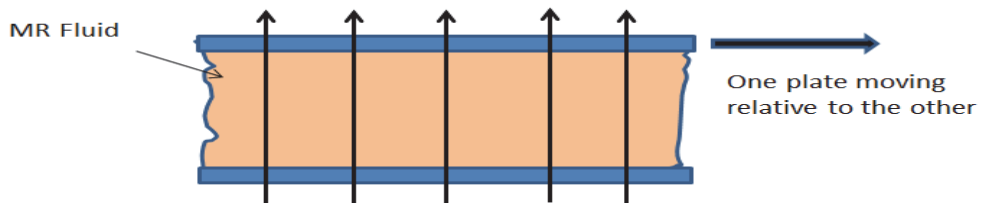


Fig. 5. Shear mode.

Squeeze-flow mode: In this mode the fluid is between two plates moving in the direction perpendicular to their planes. It is most useful for controlling small movements with large forces, see Fig. 6.

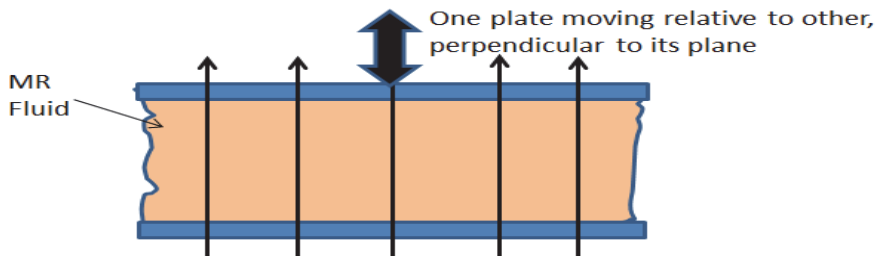


Fig. 6. Squeeze flow mode.

2.3 MR damper categories

2.3.1 Linear MR dampers

There are three main types of linear MR dampers, the mono, twin and double-ended MR dampers (Ashfak et. al, 2011). All of these have the same physical structure of an outer casing, piston rod, piston, electromagnet and the MR fluid itself.

2.3.2 Mono and twin

The mono damper is named because of its single MR fluid reservoir. As the piston displaces due to an applied force, the MR liquid compresses the gas in the gas reservoir. Just like the other two MR damper types, the mono MR damper has its electromagnets located in the piston. Fig. 7 shows a schematic diagram of the mono MR damper.

The twin MR damper has two housings, see Fig. 8. Other than this, it is identical to the mono MR damper.

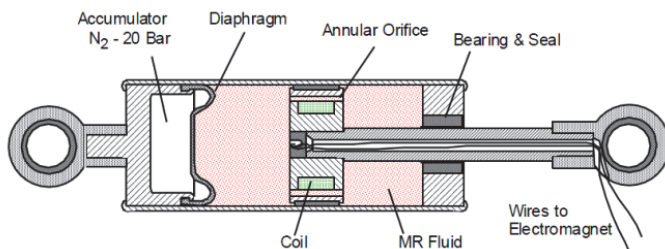


Fig. 7. The mono MR damper.

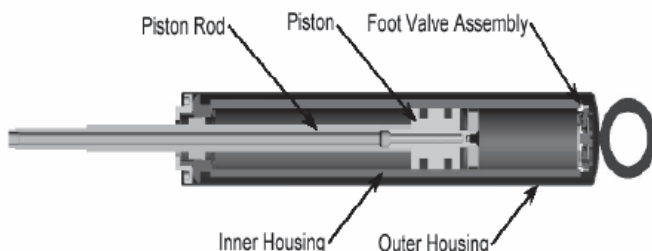


Fig. 8. The twin MR damper.

2.3.3 Double-ended

The double-ended MR damper is named so because of the double protruding pistons from both ends of the piston, see Fig. 9. No gas accumulators are used in this setup because the MR fluid is able to squeeze from one chamber to the other. In an experimental design by Lord Corp, a thermal expansive accumulator is used. This is to store the expanded liquid due to heat generation, see Fig. 10.

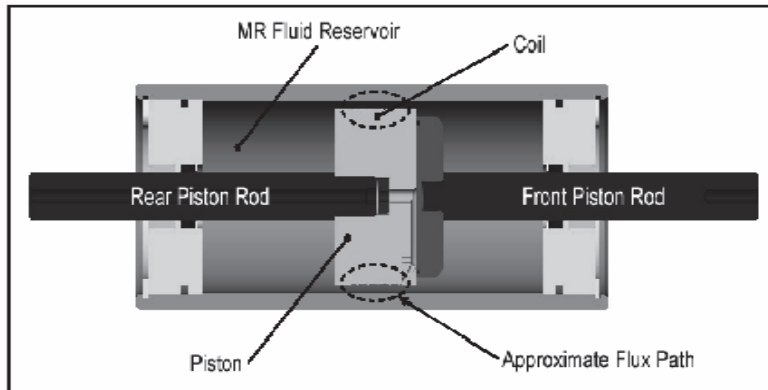


Fig. 9. Double-ended MR damper.

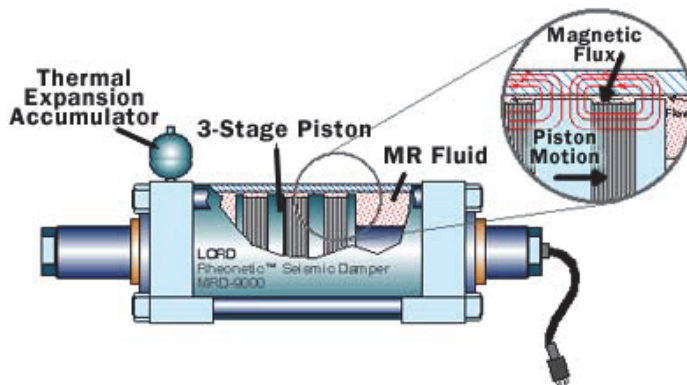


Fig. 10. Double-ended MR damper with thermal expansion accumulator.

2.3.4 Rotary dampers

Rotary dampers, as the name suggests, are used when rotary motion needs damping. There exist several types of rotary dampers, but the one that will be described is the disk brake. This is also the type that is used on the SAS platform.

The disk brake is one of the most commonly used rotary dampers. It has a disk shape and contains MR fluid and a coil as shown in Fig. 11. Different setups have been proposed for the MR disk brake. A comparison of these has been done by Wang et al (2004) and Carlson et al (1998).

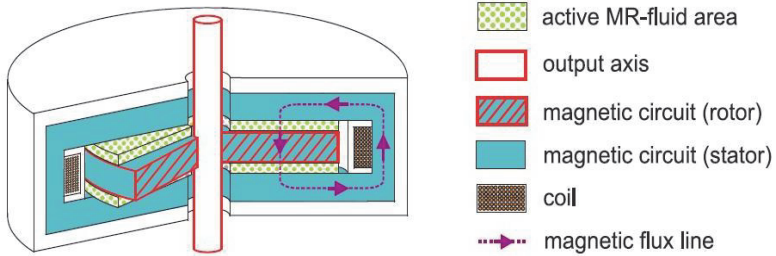


Fig. 11. MR brake disk.

3. Problem formulation

The experimental platform used in this work is fabricated by the Polish company Inteco Limited, see Fig. 12. It consists of a rocking lever that emulates the car body, a spring, and an MR damper that makes the semiactive vibration control. A DC motor coupled to an eccentric wheel is used to simulate the vibrations induced to the vehicle. Thus, the higher is the motor angular velocity, the higher is the frequency of the car (rocking lever) vibrations. The detailed definitions of the angles and distances can be found in the appendix.

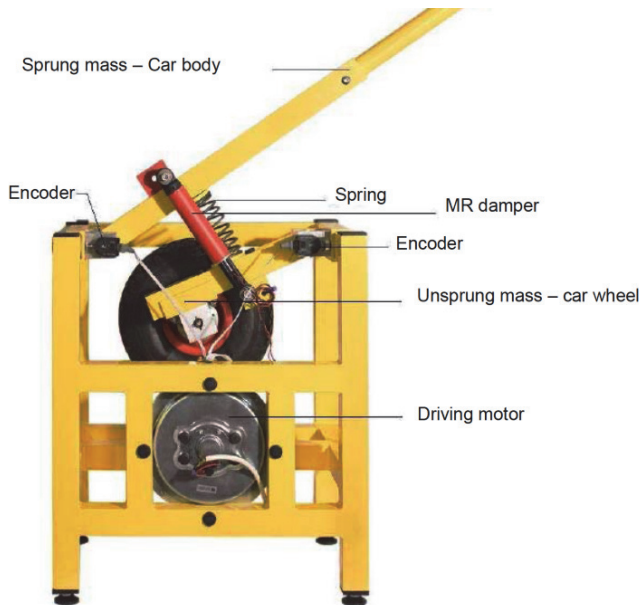


Fig. 12. Picture of the SAS system (Inteco Ltd., Poland).

The equations of motion of the upper rocking lever are given by:

$$\begin{aligned}\dot{\alpha}_2 &= \omega_2 \\ \ddot{\alpha}_2 &= J_2^{-1} (M_{21} + M_{22} + M_{s2}) + J_2^{-1} r_{2f} F_{eq} f_{mr} \sin(\pi - \alpha_{2f} - \alpha_2 - \gamma_f)\end{aligned}\quad (1)$$

where α_2 and ω_2 are the angular position and angular speed of the upper lever, respectively. M_{21} , M_{22} and M_{s2} are the viscous friction damping torque, the gravitational forces torque and the spring torque acting on the lower rocking lever, respectively and their equations are:

$$\begin{aligned} M_{21} &= -k_2 \omega_2 \\ M_{22} &= -G_2 R_2 \cos(\alpha_2) \\ M_{s2} &= r_{2s} F_s \sin(\pi - \alpha_2 + \alpha_{2s} - \gamma_s) \end{aligned} \quad (2)$$

F_s is the force generated by the spring and γ_s is the slope angle of the spring operational line, which are given by:

$$F_s = K_s \left(l_{0s} - \sqrt{(r_{2s} \sin(\alpha_2 - \alpha_{2s}) + r_{1s} \sin(\alpha_1 - \alpha_{1s}))^2 + (b - r_{1s} \cos(\alpha_1 - \alpha_{1s}) - r_{2s} \cos(\alpha_2 - \alpha_{2s}))^2} \right) \quad (3)$$

$$\gamma_s = \text{abs} \left(\tan^{-1} \left(\frac{-r_{1s} \sin(\alpha_1 - \alpha_{1s}) - r_{2s} \sin(\alpha_2 - \alpha_{2s})}{b - r_{1s} \cos(\alpha_1 - \alpha_{1s}) - r_{2s} \cos(\alpha_2 - \alpha_{2s})} \right) \right) \quad (4)$$

$F_{eq} \cdot f_{mr}$ is the force generated by the MR damper:

$$F_{eq} \cdot f_{mr} = f_{mr} (\omega_2 r_{2f} \cos\left(-\frac{\pi}{2} + \alpha_2 + \alpha_{2f} + \gamma_f\right) + \omega_1 r_{1f} \cos\left(-\frac{\pi}{2} + \alpha_1 + \alpha_{1f} + \gamma_f\right)) \quad (5)$$

$$\gamma_f = \text{abs} \left(\tan^{-1} \left(\frac{-r_{1f} \sin(\alpha_1 + \alpha_{1f}) - r_{2f} \sin(\alpha_2 + \alpha_{2f})}{b - r_{1f} \cos(\alpha_1 + \alpha_{1f}) - r_{2f} \cos(\alpha_2 + \alpha_{2f})} \right) \right) \quad (6)$$

The model is completed with the equations of motion of the lower rocking lever:

$$\begin{aligned} \dot{\alpha}_1 &= \omega_1 \\ \dot{\omega}_1 &= J_1^{-1} (M_{11} + M_{12} + M_{13} + M_{14} + M_{s1} + M_{f1}) \end{aligned} \quad (7)$$

with

$$\begin{aligned} M_{11} &= -k_1 \omega_1 \\ M_{12} &= -G_2 R_2 \cos(\alpha_2) \\ M_{13} &= -R_1 \cos(\alpha_1 + \beta) (K_g (l_0 + r + R_1 \sin(\alpha_1 + \beta) - D_x + e(t))) \\ M_{14} &= f_g \left(\frac{de(t)}{dt} - R_1 \cos(\alpha_1 + \beta) \right) \\ M_{s1} &= r_{1s} F_s \sin(\pi - (\alpha_1 - \alpha_{1s}) - \gamma_s) \\ M_{f1} &= r_{1f} F_f \sin(\pi - (\alpha_1 + \alpha_{1f}) - \gamma_f) \end{aligned} \quad (8)$$

where M_{11} is the viscous friction damping torque; M_{12} is the gravitational forces torque; M_{13} is the actuating kinematic torque transferred through the tire; M_{14} is the damping torque generated by the gum of tire; M_{s1} is the torque generated by the spring; M_{f1} is the torque generated by the damper, and $e(t)$ is the disturbance input.

The objective of the semiactive suspension is to reduce the vibrations of the car body (the upper rocking lever). This can be achieved by reducing the angular velocity of the lever ω_2 .

Thus, the system to be controlled is that of (1) by assuming that the lower rocking lever dynamics constitute the disturbances.

4. Backstepping control design

For making the backstepping control design, define z_1 and z_2 as the new coordinates according to:

$$(z_1, z_2) = (\alpha_2 - \alpha_{2equ}, \omega_2) \quad (9)$$

where the equilibrium point of the system is $(\alpha_{2equ}, \omega_{2equ}) = (0.55 \text{ rad}, 0)$, $f_{mr} = 0$. The above change of coordinates is made so that the equilibrium point is set to $(0, 0)$. In the new coordinates, (1) becomes:

$$\begin{aligned} \dot{z}_1 &= z_2 \\ \dot{z}_2 &= J_2^{-1}(M_{21} + M_{22} + M_{s2}) + J_2^{-1}r_{2f}F_{eq} \sin(\pi - \alpha_{2f} - z_1 - \alpha_{2equ} - \gamma_f) f_{mr} = f + g \cdot f_{mr} \end{aligned} \quad (10)$$

The backstepping technique can now be applied to the system (10). First, define the following standard backstepping variables and their derivatives:

$$\begin{aligned} e_1 &= z_1 & \dot{e}_1 &= z_2 \\ e_2 &= z_2 - \delta_1 & \dot{e}_2 &= \dot{z}_2 + h_1 z_2 \\ \delta_1 &= -h_1 e_1, \quad h_1 > 0 & \dot{\delta}_1 &= -h_1 z_2 \end{aligned} \quad (11)$$

For the control design, the following Bouc-Wen model of the MR damper (Ikhouane and Dyke, 2007) is used:

$$f_{mr} = \alpha(v)w + c(v)\dot{x} \quad (12a)$$

$$\dot{w} = -\gamma|\dot{x}|w|w|^n - \beta\dot{x}|w|^n + \delta\dot{x} \quad (12b)$$

$$c(v) = c_0 + c_1 v \quad (12c)$$

$$\alpha(v) = \alpha_0 + \alpha_1 v \quad (12d)$$

where v is the control voltage and w is a variable that accounts for the hysteretic dynamics. $\alpha, c, \beta, \gamma, n, \delta$ are parameters that control the shape of the hysteresis loop. From control design point of view, it is desirable to count on the inverse model, i.e., a model that predicts the control voltage for producing the damping force required to reduce the vibrations. This is because the force cannot be commanded directly; instead, voltage or current signals are used as the control input to approximately generate the desired damping force.

Now, define the following Lyapunov function candidate:

$$V = \frac{1}{2}V_1^2 + \frac{1}{2}V_2^2 = \frac{1}{2}e_1^2 + \frac{1}{2}e_2^2 \quad (13)$$

Deriving (13) and substituting (10)-(11) in the result yields:

$$\begin{aligned}\dot{V} &= e_1 \dot{e}_1 + e_2 \dot{e}_2 = e_1 e_2 - h_1 e_1^2 + e_2 f + e_2 g \cdot f_{mr} + h_1 z_2 e_2 \\ &= -h_1 e_1^2 - h_2 e_2^2 + e_2 \left[(\alpha_2 - \alpha_{2equ})(1 + h_1 h_2) + (h_1 + h_2) \omega_2 + f + g \cdot f_{mr} \right]\end{aligned}\quad (14)$$

In order to make $\dot{V}(t)$ negative, the following control law is proposed to generate the force f_{mr} :

$$f_{mr} = -\frac{(\alpha_2 - \alpha_{2equ})(1 + h_1 h_2) + (h_1 + h_2) \omega_2 + f}{g} \quad (15)$$

Substitution of (15) into (14) yields:

$$\dot{V} = -h_1 e_1^2 - h_2 e_2^2 < 0, \quad \forall h_1, h_2 > 0 \quad (16)$$

Thus, according to the Lyapunov stability theory, the system is asymptotically stable. Therefore, $e_1 \rightarrow 0$ and $e_2 \rightarrow 0$, and consequently $\alpha_2 \rightarrow \alpha_{2equ}$ and $\omega_2 \rightarrow 0$ by using the control law (15).

Note that the control force f_{mr} in (15) cannot be commanded directly, thus voltage or current commanding signals are used as the control input to approximately generate the desired damping force. Concretely, by making use of the Dahl model (12), the following voltage commanding signal is obtained from (15):

$$v(t) = \begin{cases} -\frac{(\alpha_2 - \alpha_{2equ})(1 + h_1 h_2) + (h_1 + h_2) \omega_2 + f - g(c_0 \dot{x} + \alpha_0 w)}{(\alpha_1 w + c_1 \dot{x})g} & \forall g \neq 0 \\ 0 & \text{otherwise} \end{cases} \quad (17)$$

which is the control signal that can be sent to the MR damper.

5. Simulation results

In this section, MR damper parameters $\alpha_0 = 1,8079$, $\alpha_1 = 8,0802$, $c_0 = 0,0055$, $c_1 = 0,0055$, $\gamma = 84,0253$, $\beta = 100$, $n = 1$ and $\delta = 80,7337$ (Ikhouane and Dyke, 2007) are taken for the simulation. The displacement curves and velocity curves showing hysteresis of the three last simulations, with different values of voltage, are given in Fig. 13 and Fig. 14, respectively. The blue curve is for no current, and gives the effect of the passive damper. We notice that the higher current the higher torque and less hysteresis width. All of the curves starts wide, and gets smaller and closer to zero by time. This is because of the damping. The system is stable.

Now, the backstepping control law (17) was applied to the experimental platform with the parameters $h_1 = 1$ and $h_2 = 10$ for the simulation.

The effectiveness of the backstepping controller for the vibration reduction can be seen in Fig. 15. It shows the system response (angular position and velocity) for three different excitation inputs: step, pulse train and random excitation. The figures show the comparison of the system response in two cases: “no control”, when the current to MR damper is 0 A at all times (or equivalently, the voltage is set to 0 V) and “Backstepping”, when the controller

is activated. The reduction in the RMS angular velocity achieved in each case is 43.5%, 37.3% and 40.7%, respectively.

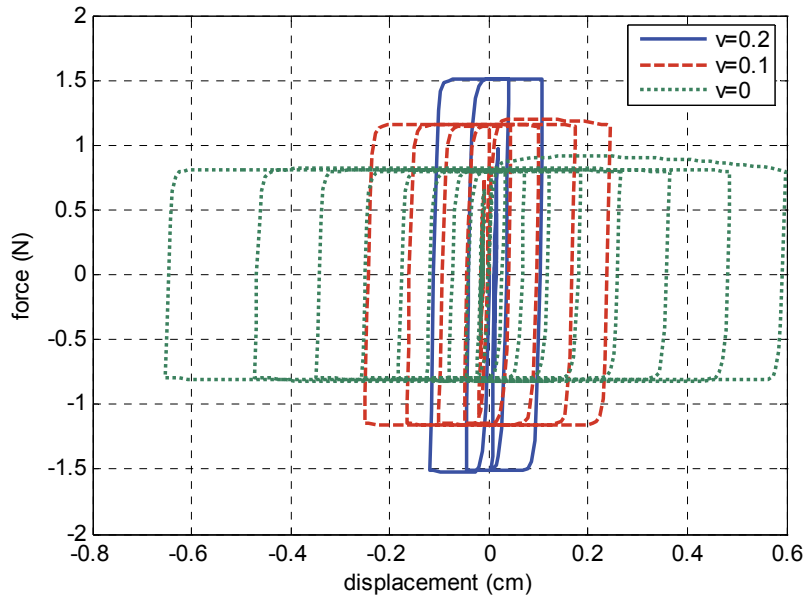


Fig. 13. Displacement vs torque.

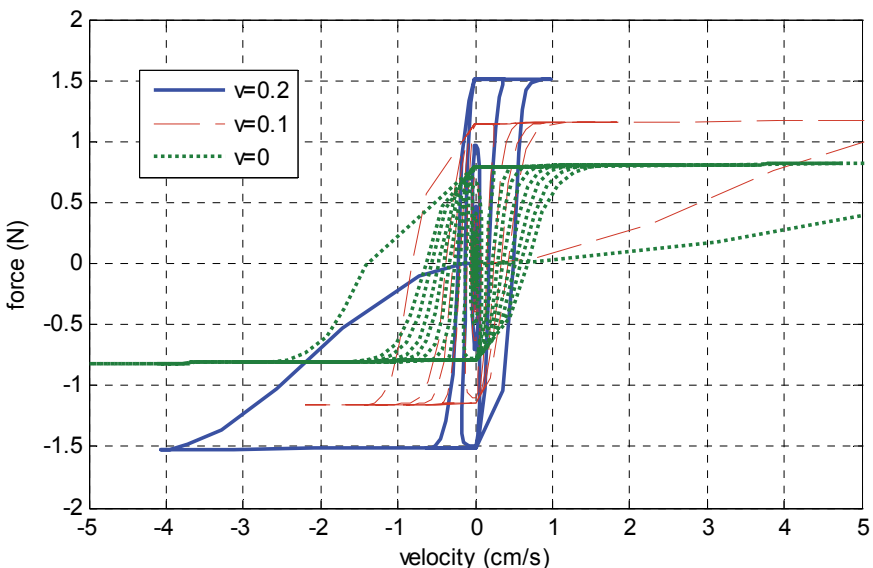
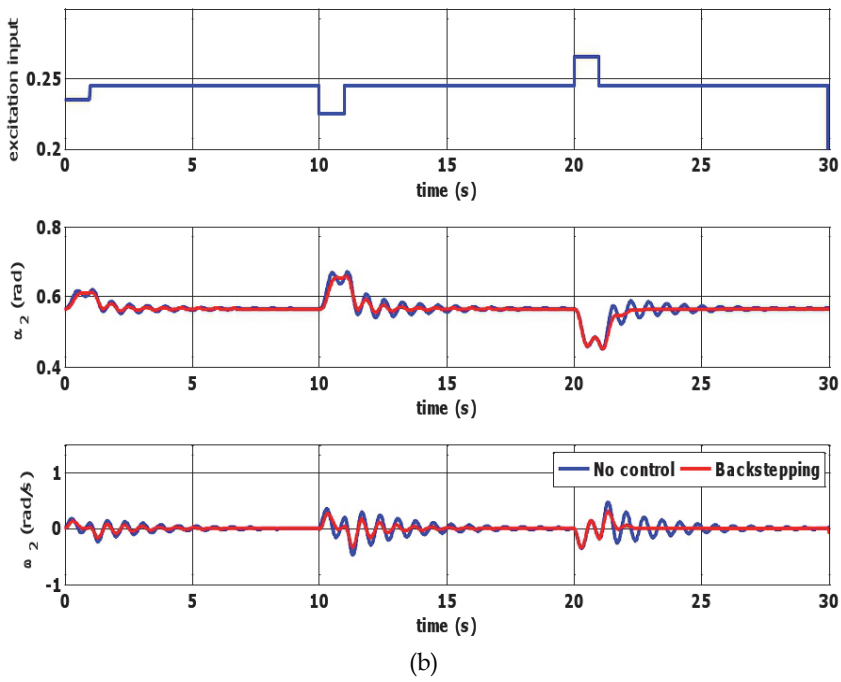
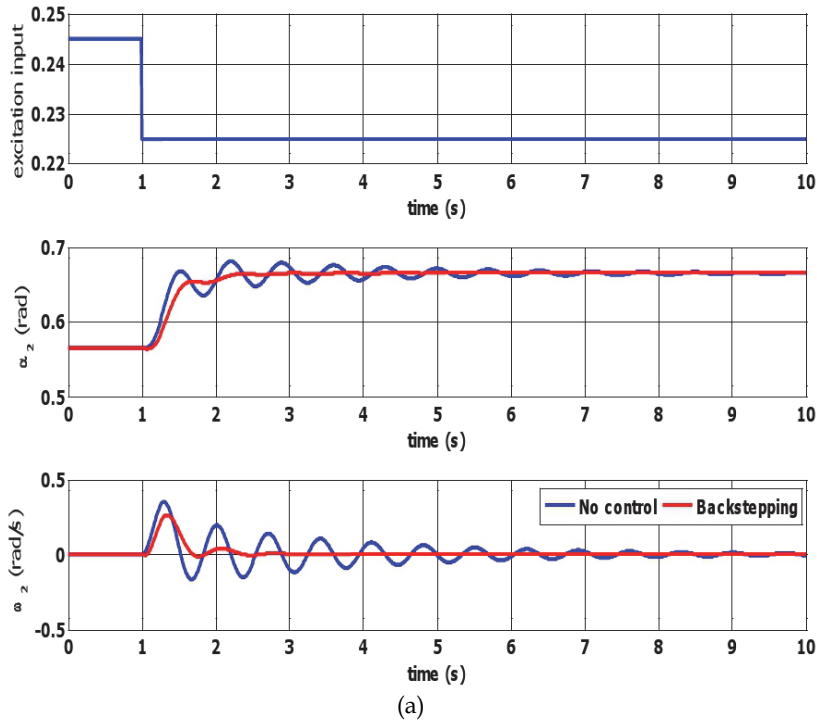


Fig. 14. Velocity vs torque.



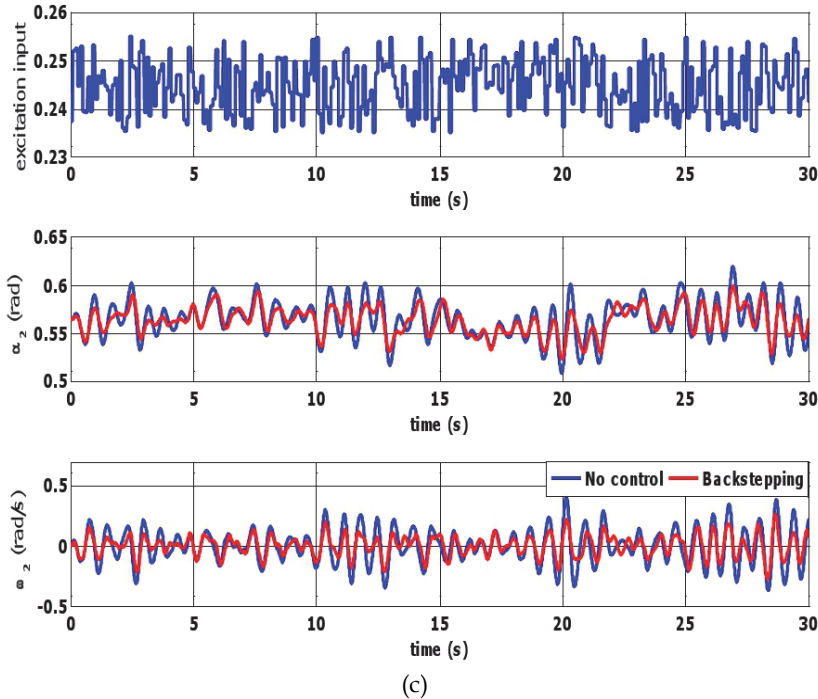
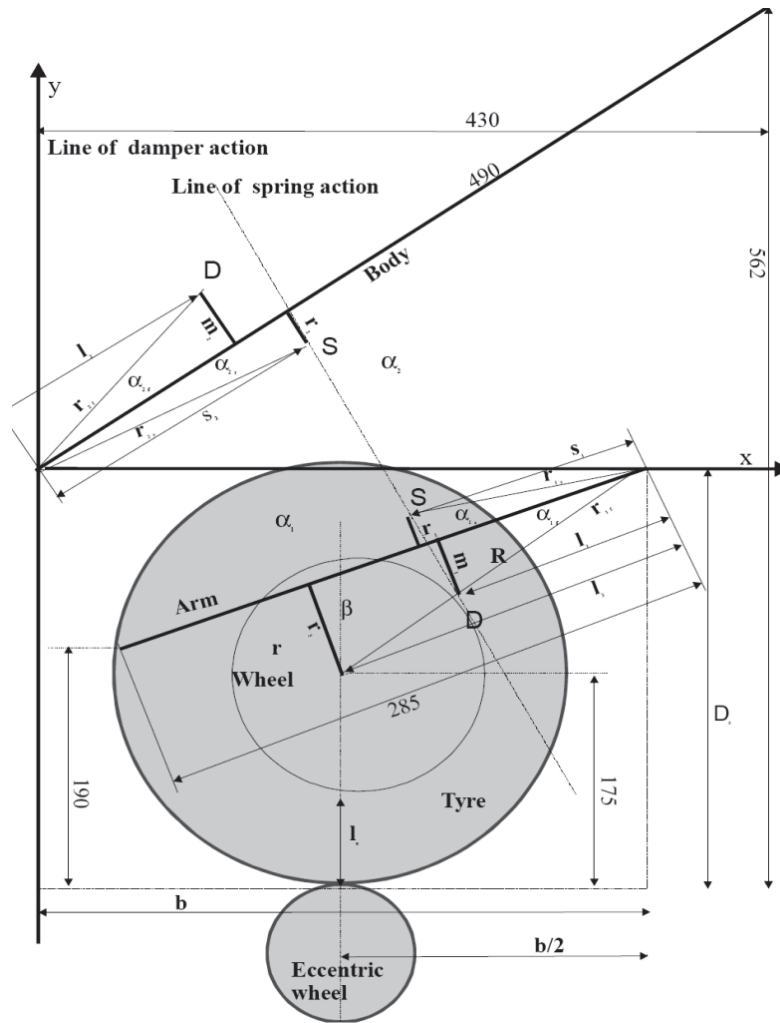


Fig. 15. Suspension systems response with the backstepping control: (a) Step input; (b) Pulse train input; (c) Random input.

6. Conclusions

In this paper we have studied the application of semiactive suspension for the vibration reduction in a class of automotive systems by using MR dampers. Backstepping and heuristic controllers have been proposed: the first one is able to account for the MR damper's nonlinearities and the second one needs only the information of the measured vibration. The control performance has been evaluated through the simulations on an experimental vehicle semiactive suspension platform. It has been shown that the proposed semiactive control strategies are capable of reducing the suspension deflection with a significantly enhanced control performance than the passive suspension system.

7. Appendix. Geometrical diagram (Inteco SAS manual)



Geometrical diagram (Inteco SAS Manual)

where

- $r_1 = r_2 = 0.025$ m: distance between the spring joint and the lower and upper rocking lever line.
- $r_3 = 0.050$ m: distance between the wheel axis and the lower rocking lever line.
- $l_1 = 0.125$ m: distance between the damper joint and the lower rocking lever line.
- $l_2 = 0.130$ m: distance between the damper joint and the upper rocking lever line.
- $l_3 = 0.200$ m: distance between the wheel axis and the lower rocking lever line.
- $s_1 = 0.135$ m: distance between the spring joint and the lower rocking lever line.
- $s_2 = 0.160$ m: distance between the spring joint and the upper rocking lever line.

- $\alpha_{1f} = 0.2730$ rad: damper fixation angle.
- $\alpha_{2f} = 0.2630$ rad: damper fixation angle.
- $\alpha_{1s} = 0.1831$ rad: spring fixation angle.
- $\alpha_{2s} = 0.1550$ rad: spring fixation angle.
- $\beta = 0.2450$ rad: wheel axis fixation angle.
- $r_{1f} = 0.1298$ m: lower rotational radius of the damper suspension.
- $r_{2f} = 0.1346$ m: upper rotational radius of the damper suspension.
- $r_{1s} = 0.1373$ m: lower rotational radius of the spring suspension.
- $r_{2s} = 0.1619$ m: upper rotational radius of the spring suspension.
- $R = 0.2062$ m: rotational radius of the wheel axis.
- $D_x = 0.249$ m: distance between the rocking lever rotational axis and the wheel bottom (minimal eccentricity).
- $r = 0.06$ m: radius of rim.
- $l_0 = 0.07$ m: tire thickness.
- $b = 0.330$ m: distance between the rocking lever rotational axis and car body.

8. References

- A. Ashfak, A. Saheed, K. K. Abdul Rasheed, and J. Abdul Jaleel (2011). Design, Fabrication and Evaluation of MR Damper. *International Journal of Aerospace and Mechanical Engineering*. 1, vol. 5, pp. 27-33.
- J.D. Carlson (1999), Magnetorheological fluid actuators, in *Adaptronics and Smart Structures. Basics, Materials, Design and Applications*, edited by H. Janocha, London: Springer.
- J.D. Carlson, D.F. LeRoy, J.C. Holzheimer, D.R. Prindle, and R.H. Marjoram. Controllable brake. *US patent 5,842,547*, 1998.
- H. Du and N. Zhang (2007), H_∞ control of active vehicle suspensions with actuator time delay, *J. Sound and Vibration*, vol. 301, pp. 236-252.
- S.J. Dyke, B.F. Spencer Jr., M.K. Sain and J.D. Carlson (1998), An experimental study of MR dampers for seismic protection, *Smart Materials and Structures*, vol. 7, pp. 693-703.
- H. Gavin, J. Hoagg and M. Dobossy (2001). *Optimal Design of MR Dampers*. Proc. U.S.-Japan Workshop on Smart Structures for Improved Seismic Performance in Urban Regions, Seattle, WA, 2001. pp. 225-236.
- E. Guglielmino, T. Sireteanu, C.W. Stammers and G. Ghita (2008), *Semi-active Suspension Control: Improved Vehicle Ride and Road Friendliness*, London: Springer.
- F. Ikhouane and J. Rodellar (2007), *Systems with hysteresis: Analysis, Identification and Control Using the Bouc-Wen Model*, West Sussex: John Wiley & Sons.
- F. Ikhouane and S.J. Dyke (2007), Modeling and identification of a shear mode magnetorheological damper, *Smart Materials and Structures*, vol. 16, pp. 1-12.
- INTECO Limited (2007), *Semiactive Suspension System (SAS): User's Manual*.
- A. Karkoub and A. Dhabi (2006), Active/semiactive suspension control using magnetorheological actuators, *Int. J. Systems Science*, vol. 37, pp. 35-44.
- A. Rodriguez, F. Ikhouane, J. Rodellar and N. Luo (2009), Modeling and identification of a small-scale magneto-rheological damper, *J. Intelligent Material Systems and Structures*, vol. 20, pp. 825-835.

- Y. Shen, M.F. Golnaraghi and G.R. Heppler (2006), Semiactive vibration control schemes for suspension system using magnetorheological damper, *J. Vibration and Control*, vol. 12, pp. 3-24.
- B.F. Spencer, S.J. Dyke, M.K. Sain and J.D. Carlson (1997), Phenomenological model of a magnetorheological damper, *ASCE J. Engineering Mechanics*, vol. 123, pp. 230-238.
- H. Wang, X.L. Gong, Y.S. Zhu, and P.Q. Zhang (2004). A route to design rotary magnetorheological dampers. In Proceedings of the Ninth International Conference on Electrorheological Fluids and Magnetorheological Suspensions, pages 680-686, Beijing, China.
- M. Zapateiro and N. Luo (2007), Parametric and non-parametric characterization of a shear mode MR damper, *J. Vibroengineering*, vol. 9, pp. 14-18.
- M. Zapateiro, N. Luo, H.R. Karimi and J. Vehi (2009), Vibration control of a class of semiactive suspension system using neural network and backstepping techniques, *Mechanical Systems and Signal Processing*, vol. 23, pp. 1946-1953.